Fermi National Accelerator Laboratory

FERMILAB-FN-587

# A Weighting Strategy for Compensating Leakage in the SDC Electromagnetic Calorimeter

A. Beretvas, D. Green, J. Marraffino and W. Wu

*Fermi National Accelerator Laboratory*
*P.O. Box 500, Batavia, Illinois 60510*

April 1992

Operated by Universities Research Association Inc. under Contract No. DE-AC02-76CHO3000 with the United States Department of Energy

## Disclaimer

# A WEIGHTING STRATEGY FOR COMPENSATING LEAKAGE IN THE SDC ELECTROMAGNETIC CALORIMETER

A. Beretvas, D. Green, J. Marraffino and W. Wu

Fermi National Accelerator Laboratory
Batavia, IL 60510

## Introduction

Econonomic constraints, among others, impose a real limit on the depth of any calorimeter. This limit may then have a corresponding effect on the performance of the device by distorting one or more of it's response, linearity and resolution. All of this applies to the calorimeter proposed by the Solenoidal Detector Collaboration, SDC, particularly since precision electromagnetic calorimetry is one of the main goals. To be sure, discussion of the effects of limited depth must take place in the context of the physics of interest since that clearly sets the scale against which detector performance is to be measured. All of this has been discussed in recent notes[1,2] on the "massless gap" technique as a way to compensate for the magnet coil between the interaction region and some calorimeter towers and the reader is referred to that note. For the present purposes, it is sufficient to note that a major design goal for the electromagnetic calorimeter is energy resolution of ~1% at the $Z^o$ mass, that being about equal to the fractional $Z^o$ natural width.

The simulation described here is a model of the SDC EM tile calorimeter consisting of 100 alternating plates of 2.5 mm thick scintillator and 3.175 mm (1/8") thick lead, representing about 25 $X_o$ (radiation lengths) of electromagnetic absorber. This model is thicker than that of the proposed EM calorimeter and serves as a benchmark "infinite" depth tower for subsequent comparisons. Upstream of the first plate (scintillator) of the tower proper are 10.68 cm of Al, representing the magnet coil, and a 30 cm air gap. The details of the entire stack are summarized in Table 1 and described in more detail below. In connection with some earlier work by this group[3] and others[4], there were existing programs to generate e/gamma showers (using EGS4) and some accompanying analysis programs for the CDF "endplug upgrade" geometry. The shower generating program has been modified to implement the SDC geometry, and the corresponding changes made in the analysis code. These were then used to study the following topics:

a) The effect of energy leakage due to the finite length of the calorimeter on the resolution and it's compensation by weighting the last three layers of readout.

b) The energy dependence of the weight factors obtained in the above study.

c) The shower angle dependence of the weight factors obtained in the above study.

Table 1. Model Tower Stack Geometry

| Element Number | $Z_{begin}$ (cm) | Thickness (cm) | $Z_{end}$ (cm) | Active Number | Inert Number | Material |
|---|---|---|---|---|---|---|
| 1 | 0.0000 | 170.0000 | 170.0000 | | 1 | air (NTP) |
| 2 | 170.0000 | 10.6800 | 180.6800 | | 2 | aluminum coil |
| 3 | 180.6800 | 30.0000 | 210.6800 | | 3 | air (NTP) |
| 4 | 210.6800 | 0.2500 | 210.9300 | 1 | | scintillator |
| 5 | 210.9300 | 0.3175 | 211.2475 | | 4 | lead |
| 6 | 211.2475 | 0.2500 | 210.9300 | 2 | | scintillator |
| 7 | 211.4975 | 0.3175 | 211.8150 | | 5 | lead |
| 8 | 211.8150 | 0.2500 | 212.0650 | 3 | | scintillator |
| 9 | 212.0650 | 0.3175 | 212.3825 | | 6 | lead |
| 10 | 212.3825 | 0.2500 | 212.6325 | 4 | | scintillator |
| . | . | . | . | | | . |
| . | . | . | . | | | . |
| . | . | . | . | | | . |
| 90 | 235.0827 | 0.2500 | 235.3327 | 44 | | scintillator |
| 91 | 235.3327 | 0.3175 | 235.6502 | | 47 | lead |
| 92 | 235.6502 | 0.2500 | 235.9022 | 45 | | scintillator |
| 93 | 235.9002 | 0.3175 | 236.2177 | | 48 | lead |
| 94 | 236.2177 | 0.2500 | 236.4677 | 46 | | scintillator |
| 95 | 236.4677 | 0.3175 | 236.7852 | | 49 | lead |
| 96 | 236.7852 | 0.2500 | 237.0352 | 47 | | scintillator |
| 97 | 237.0352 | 0.3175 | 237.3527 | | 50 | lead |
| 98 | 237.3527 | 0.2500 | 237.6027 | 48 | | scintillator |
| 99 | 237.6027 | 100.0000 | 337.6028 | | 51 | vacuum |

## The SDC Geometry and the Generated Shower File

In order to simplify the problem, we have implemented the SDC EM calorimeter geometry as follows:

The coordinate system is chosen such that the z axis is normal to the calorimeter tower plates with z = 0 at the interaction point. In increasing order of z, the kinds and amounts of materials encountered are: 170 cm of air, the 1.2 $X_0$ magnet coil (namely 10.68 cm Al), then another 30 cm of air followed by the tower itself consisting of 2.5 mm scintilator plates alternating with 3.175 mm Pb plates. We have chosen 50 scintillator/lead pairs (100 layers) as an approximation to an "infinite" length calorimeter. To avoid a number of complications that are not relevant to this study, we consider the transverse dimensions of the tower as infinite.

Generating EGS showers is very CPU time consuming. On the other hand, we need enough statistics. As a compromise, we use 300 events for 12.5 and 25

GeV showers, and 200 (or less) events for 50 GeV and 100 GeV showers. A few 150 GeV showers were also generated for a related study but we defer discussion. To avoid having to generate all these showers repeatedly, we have recorded all the relevant variables including the position, identity and energy deposit for each electron, positron and photon in each plate for each shower. All succeeding analysis runs then simply "play back" those files and accumulate the energy sums over all particles and all plates up through some designated cut-off plate. Note that this technique is similar to another recent study [5] in which real data was used.

Limited Length of Calorimeter

Figs. 1 and 2 show the longitudinal profile of energy deposited in the active layers as a function of layer number in the benchmark tower described above for the worst leakage case of 100 GeV at normal incidence and the best case of 12.5 GeV at 60 degrees to the normal respectively. Truncating the tower at some given layer number leads to an amount of leakage energy that is equal to the sum of all bins with larger layer numbers. Recalling that the current SDC design calls for a total of 72 layers[6], we can immediately extract the following. The fractional energy leakage in a detector of 72 layers relative to the total energy deposit in a detector of 100 layers (at normal incidence) is shown in Table 2.

Table 2. Fractional Energy Leakage in a Truncated Tower for Normal Incidence Showers

| Shower Energy (GeV) | Percentage energy leakage | Position of shower-max (layer number) | Ratio of energy in last layer to energy in shower-max layer |
|---|---|---|---|
| 12.5 | 1.27% | 10 | 4.02% |
| 25.0 | 1.60% | 12 | 5.54% |
| 50.0 | 2.19% | 14 | 7.79% |
| 100.0 | 2.74% | 16 | 9.79% |

For off-normal incidence, the calorimeter appears thicker (and coarser) and there is correspondingly less energy leakage. Given that and our objective of studying various strategies for weighting the last few active elements to compensate for whatever leakage does occur, we must necessarily truncate the tower early enough to actually have some leakage to study. Thus, for showers incident at 60 degrees to the normal and with the tower truncated after layer 42, we obtain the results shown in Table 3.

Table 3. Fractional Energy Leakage in a Truncated Tower for Off-normal Incidence Showers

| Shower Energy (GeV) | Percentage energy leakage | Position of shower-max (layer number) | Ratio of energy in last layer to energy in shower-max layer |
|---|---|---|---|
| 12.5 | 1.24%(*) | 10 | 2.98%(*) |
| 25.0 | 1.62% | 12 | 3.78% |
| 50.0 | 1.84% | 14 | 4.49% |
| 100.0 | 2.52% | 16 | 4.93% |

(*) For the 12.5 GeV showers, the tower was truncated after 32 layers.

Our goal is to weight the readout from the last three layers in order to compensate for the energy leakage while keeping the energy resolution as close as possible to the case with an "infinite" length calorimeter. In contrast to Jones [5], we have chosen to apply weight factors to the last three active layers. This is based on our observation that the shape of the energy spectrum for the last layer alone is substantially different, having a longer high-side tail, from that of the total leakage spectrum. This is most likely attributed to fluctuations. If we are to have any chance of compensating for the leakage by a weighting strategy, we need to weight something whose spectrum more nearly matches the shape of the leakage spectrum. The sum (or, equivalently, the average) of the last three layers does that, at the cost of having to determine three weight factors rather than just one. Using a histogram of the integral of the energy deposit by layer of detector and some simple geometric calculations, we can construct a constraint for the three weights, thereby reducing the task to determining two weight factors.

For 50 GeV showers at normal incidence for example, the constraint formula is:

$$32 * W_3 + 30 * W_2 + 14 * W_1 = 272 * f \qquad (1)$$

where:

f is the percentage of compensation required by the leakage.

$W_3$ is the weight for the 3rd last layer,

$W_2$ is the weight for the 2nd last layer,

$W_1$ is the weight for the last layer.

Similar expressions apply to the cases of 12.5 GeV, 25 GeV and 100 GeV showers.

If the mean energy deposit in the detector is less than the mean energy deposit in the "infinite" length calorimeter, we call it "under-weighted". Otherwise, if the mean value is larger than mean value in the "infinite" case, we call it "over-weighted". There is an optimum weight combination in which the energy resolution is very close to the "infinite" case for 12.5 GeV, 25 GeV, 50 GeV and 100 GeV showers. That set of weights was chosen by examining many trials with different weight combinations. It may be that the best combination is not unique. We have tested many possibilities, and obtained the results in Table 4. For comparison, we show the resolution for the infinite tower in the last column of the table. We emphasize that, up to this point, the only criterion imposed was to reproduce the mean and width of the infinite tower energy response. There are, however, other criteria to be considered.

One of these other important issues is the linearity of the weighted tower. Define E(w) to be the total energy deposited in the detector after weighting, and $E_0$ to be the total energy deposited in the unweighted benchmark detector. We take the quantity $[E(w)-E_0]/E_0$ as a measure of the nonlinearity. Table 5 shows this quantity for different weight cases. Note that the case with the best weight, judged solely on the basis of energy resolution, also has a very small value for the nonlinearity, typically less than than 1%. However the case with the smallest nonlinearity, namely the case with the mean value very close to the mean value of the infinite case, does not always correspond to the best resolution.

It is in this context that the 150 GeV showers mentioned earlier are relevant. These events were generated as part of an attempt to find a more systematic way to determine the weight factors for the last three active elements of the calorimeter stack. Again, the criteria used were to reproduce the mean and width of the infinite tower response. To do that, we defined a chi-squared like quantity with the three weight factors as free parameters and whose minimum satisfied the mean and width criteria. Let the mean energy of the infinite tower be denoted by $E_0$ with error $dE_0$, and the corresponding mean energy for the truncated tower be E(w) with error dE(w), where w represents the set of weight factors. Similarly, let $G_0$ and $dG_0$ be the ratio of width to mean energy, and its error, for the infinite tower and G(w) and dG(w) be the same ratio and error for the truncated tower. Then the weights were chosen as those values that minimize the function

$$D = \{[E(w) - E_0]/dE\}^{**}2 + \{[G(w) - G_0]/dG\}^{**}2 \qquad (2)$$

summed over all showers. There are two things wrong with this approach as formulated. The first is that it does not use the constraint among the three weight factors but treats them as fully independent. The second is that there is no consideration of any induced nonlinearity. Since neither of these flaws is insurmountable, this approach should be pursued but has been dropped for the time being.

## A Generalization of Weighting Strategies

An an example of the use of weighting strategies to investigate some less obvious problems, we have considered the effect of a particular type of

physical damage to a tile calorimeter and its effect on energy response and resolution.

Suppose there are some readout channels of the EM calorimeter for which no signal appears for various reasons. We get no signal from these channels, even though the material is still present and contributes normally to shower development. To simulate the effect of that, we simply assign a weight of zero to some selected channel, and see how much the resolution is degraded by the loss of this channel. The worst case is that the dead channel corresponds to the otherwise active layer nearest shower-max.

For this purpose, we use the same simulations as discussed above. In addition, we assign a weight of 0.0 to layer 22 for the 12.5 GeV case, layer 26 for the 25 GeV case and layer 32 for the 100 GeV case. These layer numbers correspond to shower-max for each incident energy.

Figs. 3 and 4 show the longitudinal distribution of shower energy deposit with the best weight combination as discussed earlier without a "broken" channel, and with a "broken" channel at layer of 22 where the shower-max is located for incident energy 12.5 GeV. One can see there is a missing point in Fig. 4 at the peak of the distribution. Figs. 5 and 6 show the distribution of the total energy deposited in the detector, without and with the broken channel. We note that the peak of the plot with the broken channel is shifted to smaller energy, and the energy resolution is larger (i. e., worse) than the case without the broken channel. We summarize the results for all three incident energies in Table 6.

Table 6. Degraded Response due to a Dead Channel - Worst Case

| Incident energy GeV | Best weight combination Front/rear/total layers | Shower-max layer number | Broken Channel | Fractional Energy Deposit Mean (%) | Sigma (%) | Sigma/ Mean (%) | Ratios Mean (y/n) Sigma/mean (y/n) |
|---|---|---|---|---|---|---|---|
| 12.5 | 3.0/ 3., 2., 1./72 | 22 | No | 6.82 | 0.23 | 3.39 | 0.94/1.17 |
| 12.5 | 3.0/ 3., 2., 1./72 | 22 | Yes | 6.41 | 0.25 | 3.97 | |
| 25 | 2.0/ 2., 2., 2./72 | 26 | No | 6.81 | 0.17 | 2.48 | 0.94/1.20 |
| 25 | 2.0/ 2., 2., 2./72 | 26 | Yes | 6.40 | 0.19 | 2.99 | |
| 100 | 1.2/ 4., 3., 2./72 | 32 | No | 6.93 | 0.09 | 1.37 | 0.94/1.18 |
| 100 | 1.2/ 4., 3., 2./72 | 32 | Yes | 6.54 | 0.11 | 1.62 | |

From the above table, we see that, in the case of one channel broken at shower-max, the total energy deposit is reduced by about 6% and the fractional

resolutions are reduced by about 17%, 20% and 18% respectively for the three selected incident energies as compared to the case without a broken channel. The numbers are nearly energy independent because the broken channel has always been chosen at the location of shower-max.

A more complex issue is what happens if some channel is not completely dead but also not fully functional. This can occurr for a number of reasons such as radiation damage, a bad contact, a damaged optical fiber, or a bad photomultiplier. There could be physical damage affecting either the production or transmission of light, as well as fluctuations in the longitudinal development of individual showers. In the general case, it may be possible to address this problem by introducing a correction factor for each active layer of the detector based on the expected response as predicted by simulation. Clearly the worst case is that where we get no signal at all since no finite weight can correct for a true zero response. As as estimate of the effect of that, we have considered the case of one dead channel at shower-max.

## Conclusion

It is possible to nearly recover the energy resolution of an infinite tower in spite of the effect of the magnet coil materials and the effect of punch through. The first effect can be compensated with the "massless gap" technique of weighting the first layer readout. The second effect can also be compensated by assigning weights to the rear layers of the calorimeter. Both of these can be accomplished without significant resolution loss or the introduction of unacceptable nonlinearity.

## References


1. J. Marraffino et al, "Massless Gaps" for Solenoid + Calorimeter, FNAL TM-1766, November, 1991.

2. Effect of Dead Material to the Electro-Magnetic Calorimeter and Energy/Resolution Recovery with "Massless Gap", Hideo Hirayama, KEK Note 406.

3. J. Marraffino. EGS Study of Scintillator Thickness Variation For a Tile Calorimeter, 30 July 1991, SDC-F-90, Fermilab.

4. Qun Fan and S. L. Olsen, Effect of Longitudinal and Transverse Variations on the Energy Resolution of an Electromagnetic Sampling Calorimeter, 2 Aug. 1991, The University of Rochester.

5. L. W. Jones, Reduction of Calorimeter Depth by Weighting Last Layer, July 1991, UM HE 91-27.

6. Fermilab SDC Tile/Fiber Calorimeter Group. Calorimeter Conceptual Design, Tile/Fiber Scintillator Option, Sep. 3, 1991.

Figure Captions

1. Longitudinal energy deposit profile for normal incidence 100 GeV electrons in the "infinite" tower model calorimeter stack. Only the active layers are shown.

2. Longitudinal energy deposit profile in the "infinite" tower model calorimeter stack for 12.5 GeV electrons incident at 60 degrees to the stack normal. Only the active layers are shown.

3. Longitudinal energy deposit profile in a truncated tower for 12.5 GeV electrons at normal incidence using the best weights for the first and last three active layers. All active layers are present.

4. Longitudinal energy deposit profile in a truncated tower for 12.5 GeV electrons at normal incidence using the best weights for the first and last three active layers. Active layer 22 has been given a weight of 0.0 to simulate a dead readout.

5. Total energy deposit corresponding to the case described in Fig. 3. A gaussian fit is shown overlaid on the data. The parameters of that fit are given in the inset.

6. Total energy deposit corresponding to the case described in Fig. 4. A gaussian fit is shown overlaid on the data. The parameters of that fit are given in the inset.

Table 4. Best Weight Combinations

| Shower Energy (GeV) | Angle to Normal (degrees) | Weight for first layer | Weight for last three layers | Last Layer Number | Non-linearity (percent) | Energy Resolution using these weights for both the first and last three layers | Previous column times sqrt $E_t$ | Sqrt $E_t$ * dE/E for the "infinite" tower |
|---|---|---|---|---|---|---|---|---|
| 12.5 | 60 | 3.0 | 3. 2. 1. | 32 | 0.32 | 0.0464 | 0.116 | 0.110 |
| 12.5 | 0 | 2.0 | 3. 2. 1. | 72 | 0.06 | 0.0339 | 0.120 | 0.118 |
| 25 | 60 | 2.0 | 1. 1. 1.5 | 42 | 1.4 | 0.0345 | 0.122 | 0.119 |
| 25 | 0 | 2.0 | 2. 2. 2. | 72 | 0.3 | 0.0248 | 0.124 | 0.113 |
| 50 | 60 | 2.0 | 1. 2. 3. | 42 | 0.53 | 0.0237 | 0.118 | 0.109 |
| 50 | 0 | 1.5 | 3. 2. 1. | 72 | 0.61 | 0.0172 | 0.121 | 0.121 |
| 100 | 60 | 1.5 | 4. 5. 6. | 42 | 0.88 | 0.0159 | 0.112 | 0.105 |
| 100 | 0 | 1.2 | 4. 3. 2. | 72 | 0.95 | 0.0136 | 0.136 | 0.109 |

Table 5. Nonlinearity and Resolution vs. Shower Energy at Fixed Weight 2 on the first Weighted Layer

| Shower Energy (GeV) | Shower Angle to Normal (degrees) | Fractional Weighted (%) | Energy Deposit Benchmark (%) | $(E(w)-E_0)/E_0$ | sqrt $E_t$ | dE/E | (dE/E)*sqrt $E_t$ |
|---|---|---|---|---|---|---|---|
| 12.5 | 60 | 6.67 | 6.87 | -0.0298 | 2.5 | 0.047 | 0.118 |
| 12.5 | 0 | 6.86 | 6.87 | -0.0025 | 3.54 | 0.033 | 0.118 |
| 25 | 60 | 6.75 | 6.87 | -0.0179 | 3.54 | 0.034 | 0.119 |
| 25 | 0 | 6.84 | 6.87 | -0.0050 | 5. | 0.023 | 0.112 |
| 50 | 60 | 6.83 | 6.87 | -0.0056 | 5. | 0.022 | 0.109 |
| 50 | 0 | 6.86 | 6.87 | -0.0017 | 7.07 | 0.017 | 0.121 |
| 100 | 60 | 6.84 | 6.87 | -0.0048 | 7.07 | 0.018 | 0.128 |
| 100 | 0 | 6.87 | 6.87 | 0. | 10. | 0.012 | 0.124 |

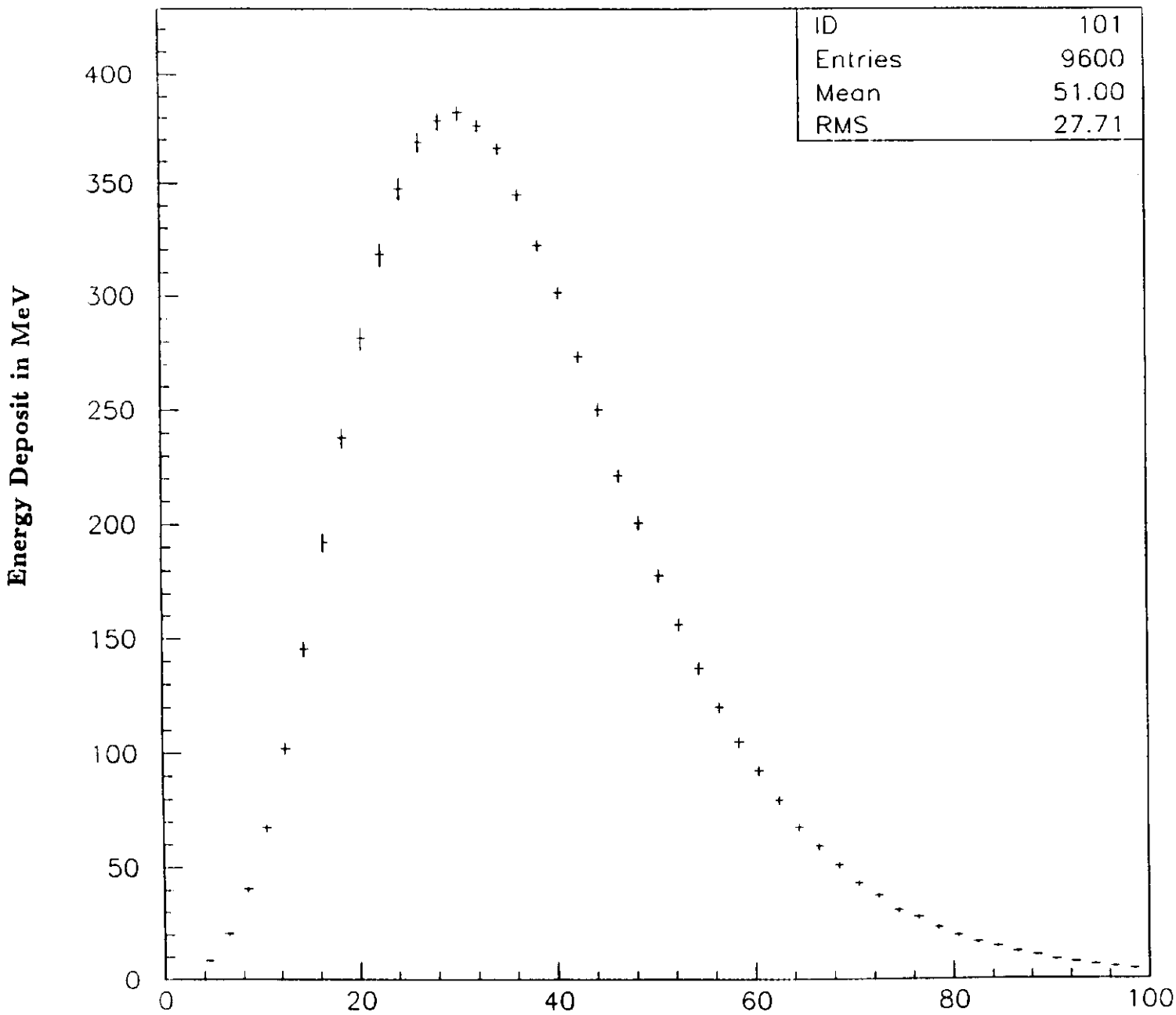


**Figure 1** **Active Layer Number**

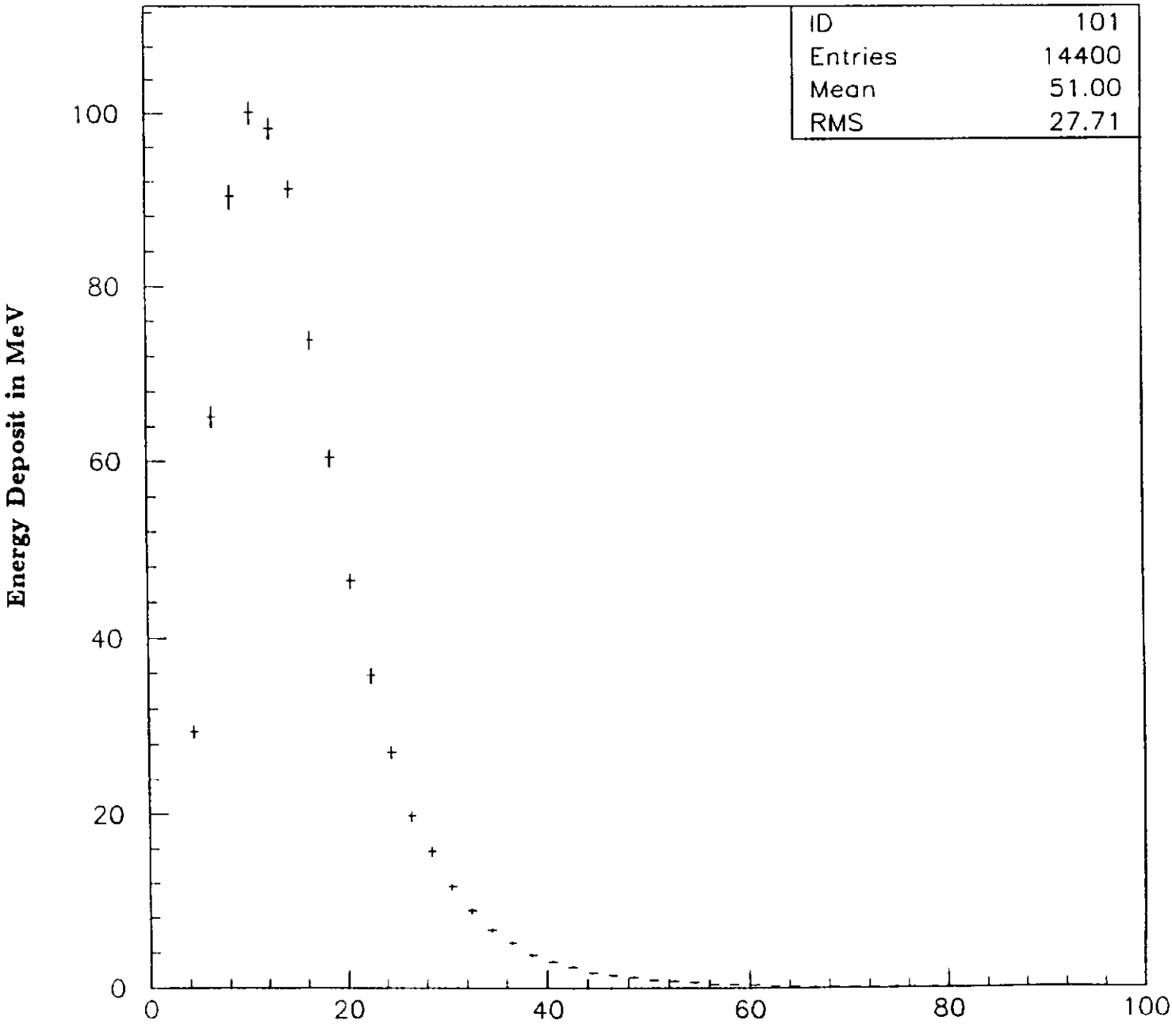


**Figure 2 Active Layer Number**

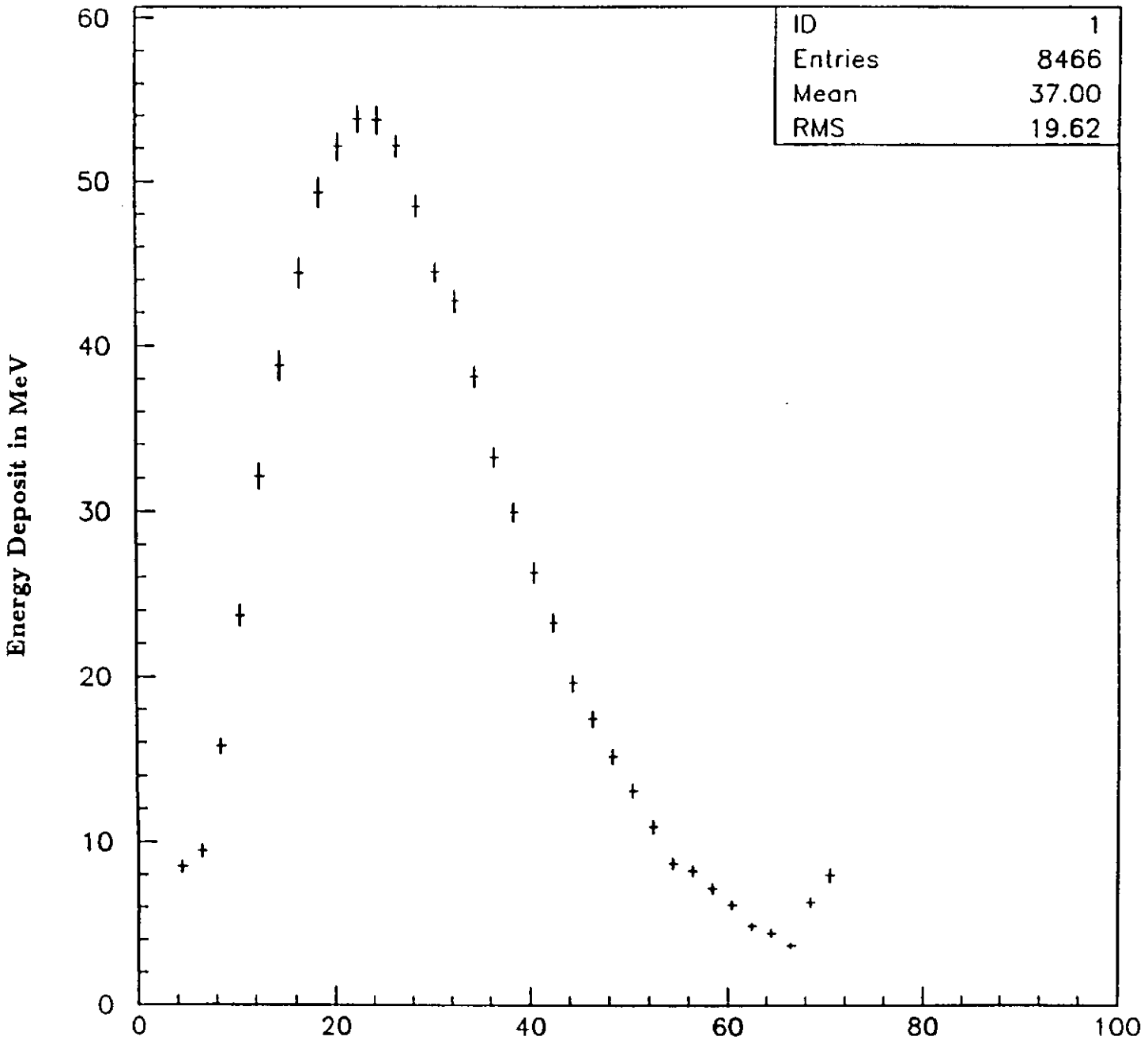


**Figure 3 Active Layer Number**

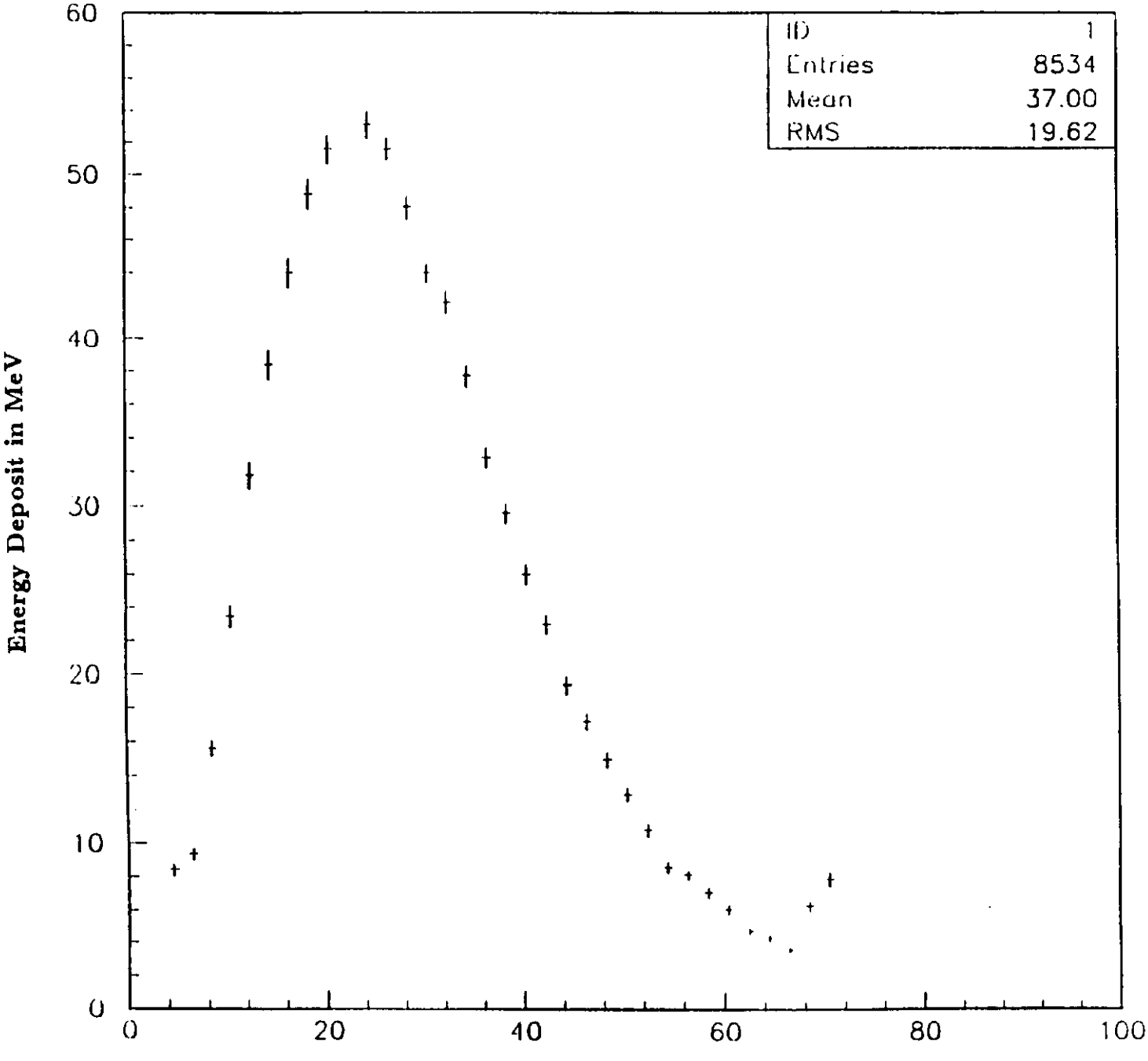


**Figure 4** **Active Layer Number**

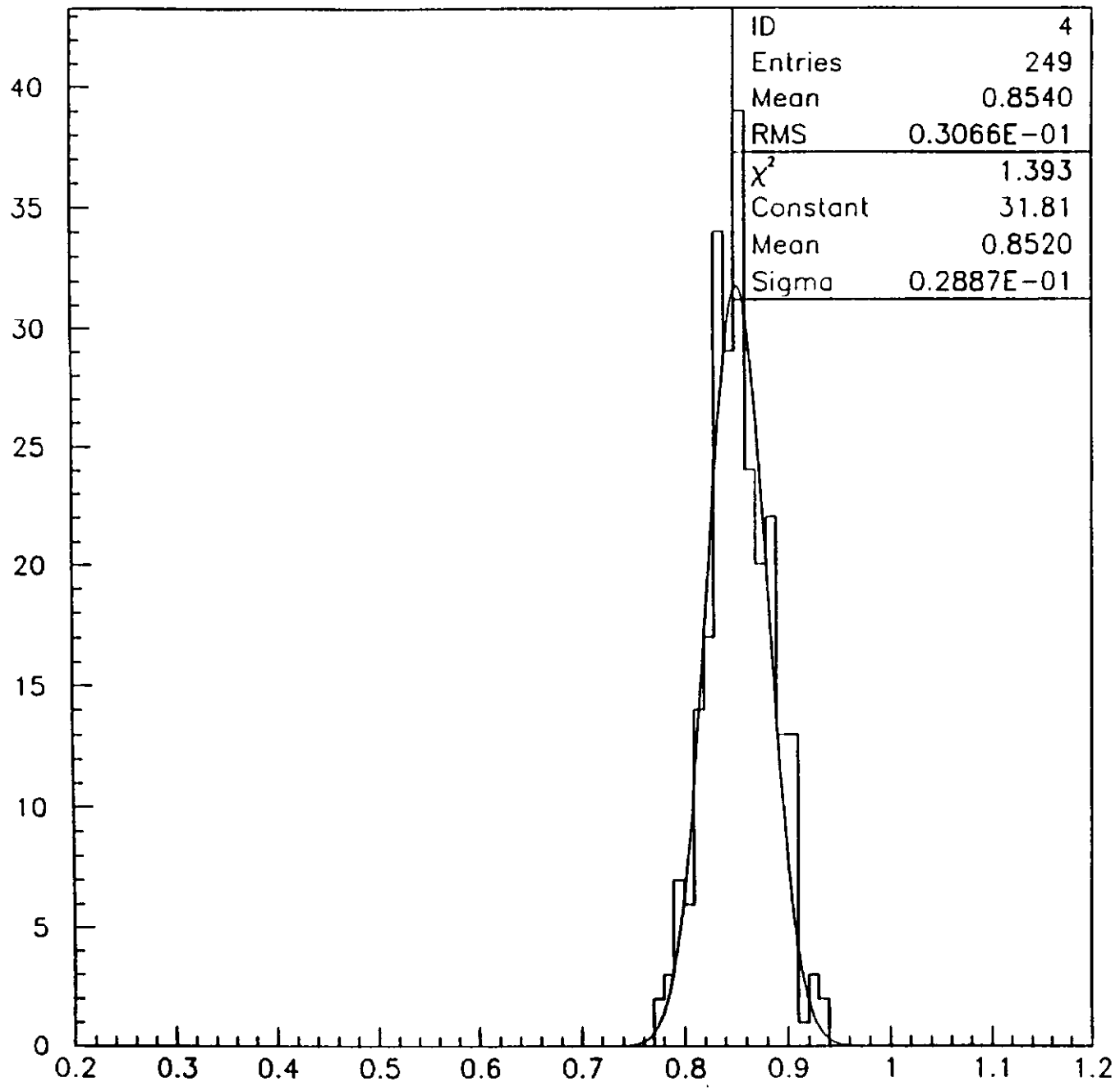


**Figure 5** **Total Energy Deposit in GeV**

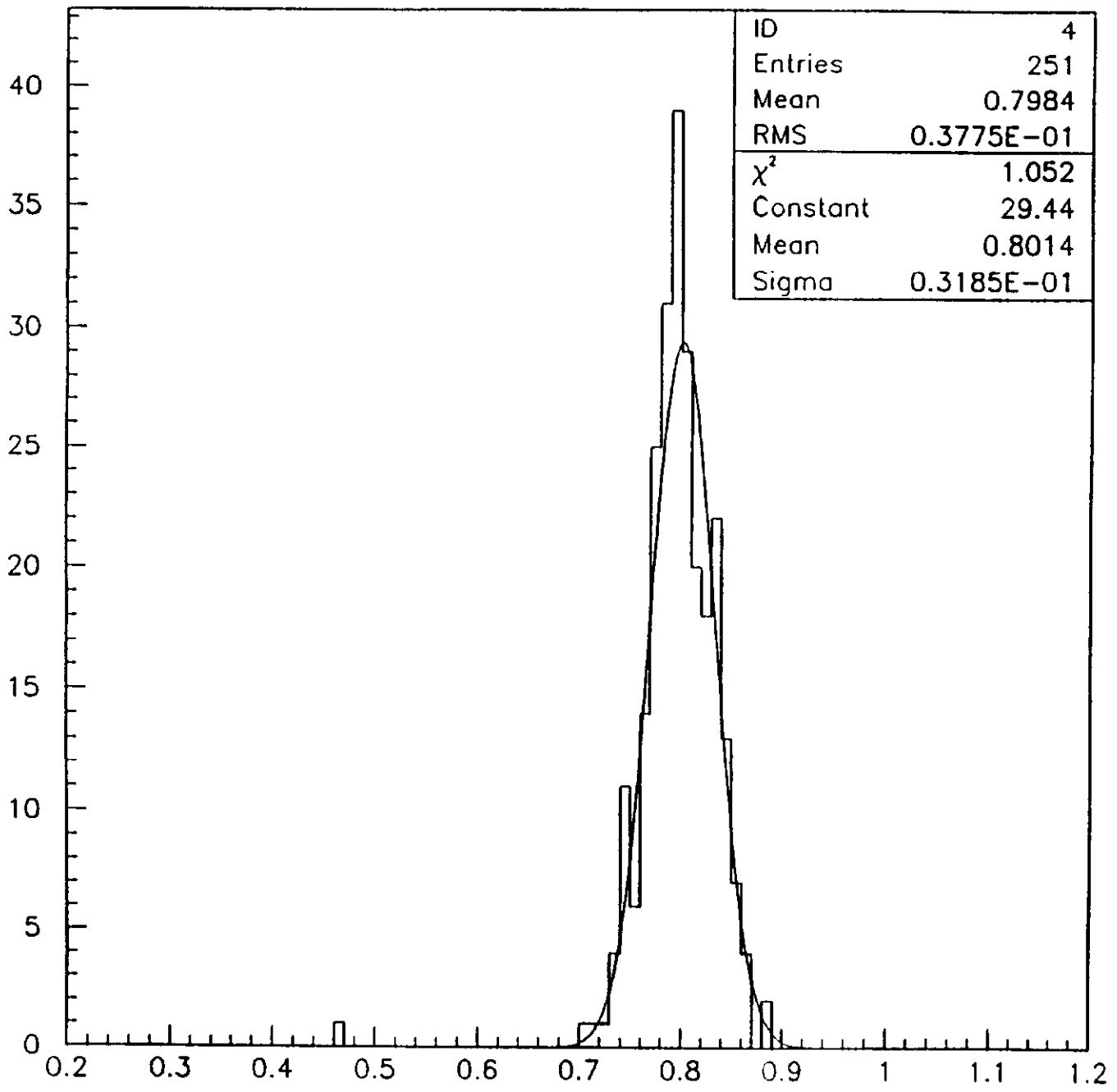


**Figure 6** **Total Energy Deposit in GeV**